ELSEVIER

Journal of Organometallic Chemistry 510 (1996) 71–81

Journal of Organometallic Chemistry

How bridging ligands and neighbouring groups tune the gold–gold bond strength

Luis F. Veiros [a], Maria José Calhorda [b,*]

[a] *Centro de Química Estrutural, Instituto Superior Técnico, 1096 Lisboa Codex, Portugal*

[b] *Instituto de Tecnologia Química e Biológica, R. da Quinta Grande, 6, Apart. 127, 2780 Oeiras, Portugal and Instituto Superior Técnico, Lisboa, Portugal*

Received 5 June 1995

Abstract

Gold-gold interactions in small polynuclear complexes are analysed using extended Hückel calculations. They are influenced by the nature of the ligand donor atoms, by the bridging ligands, but most by the formal oxidation state of the metal. Au–Au bonds are much stronger in complexes of Au(II) and Au(III), but a weak interaction between two d^{10} centres exists for Au(I) complexes, owing to mixing of the s and p orbitals with the d orbitals. Phosphines induce stronger metal–metal bonds when coordinated *trans* to the Au–Au bond in $[Au(II)[(CH_2)_2PPh_2]L]_2$ (Ph = phenyl), but have the opposite effect when bonded orthogonally to the metal–metal axis in Au(I) binuclear species. When two gold atoms are bridged by a single carbon atom, belonging either to mesityl (Mes = 2,4,6-$Me_3C_6H_2$) or CR_2, the former produces stronger Au(I)–Au(I) interactions, reflected in shorter distances. Formal oxidation states are proposed for the gold atoms in two mixed-valence clusters, $[Au_4(C_6F_5)_2\{(PPh_2)_2CH\}_2(PPh_3)_2](ClO_4)_2$ and $[\{(2,4,6\text{-}C_6F_3H_2)Au(CH_2PPh_2CH_2)_2Au\}_2\text{-}Au(CH_2PPh_2CH_2)_2Au](ClO_4)_2$. The results suggest a higher oxidation state for the outer gold atoms, in both the T-shaped tetranuclear cluster and the Au_6 linear chain.

Keywords: Gold; Metal–metal bonds; Extended Hückel calculations; Bond lengths and strengths; Bridging ligands

1. Introduction

Gold organometallic chemistry has been growing in recent years and much structural information is available [1]. Among the gold complexes, there are a significant number of Au(I) compounds. These exhibit a fairly regular pattern, showing the tendency for a linear L–Au(I)–L coordination around each gold atom, where L can be a carbon, a sulphur or a phosphorus donor. This linear arrangement can, of course, be forced to distort by geometrical factors, either steric constraints of the molecule as a whole, or the ligand coordination characteristics, such as the bite angle for bidentate species. Metal–metal interactions between different AuL_2 fragments of the molecule can also be responsible for disrupting the ideal linear coordination around each gold atom.

The existence of short Au(I)–Au(I) distances in a complex is normally associated with two main factors. One is the presence of neighbouring L–Au–L units, arising from the cyclic geometry of the molecule **1a**. The other arises when these fragments share a common ligand, R. The bridge may be a single atom **1b** or more.

The two gold atoms in **1a** may also be regarded as being bridged by two ligands, while those of **1b** are bridged by only one ligand. Unsupported Au–Au bonds are very seldom observed, and we have studied them previously [2].

The binuclear gold(I) phosphorus complex $[\{Au\{(CH_2)_2PPh_2\}\}_2]$ is one of the simplest examples of type **1a** [3]. There are a number of examples of **1b**-type complexes with a single atom bridging AuL units, some resulting in hypercoordinated species [4]. Some of these complexes have ligands R with one carbon atom bridging only two AuL fragments. These R ligands may coordinate to gold through a tetrahedral carbon atom, as in CX_2, or through an sp^2 aromatic carbon atom, as in the mesityl group (2,4,6-$Me_3C_6H_2$,Mes). The most striking example of the latter type is the all-symmetrical gold star complex $[\{Au(Mes)\}_5]$ [5], in which gold atoms

* Corresponding author.

SSDI 0022-328X(95)05860-5

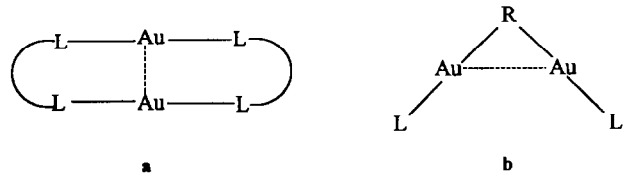

1

are bridged by Mes, in a cyclic arrangement, resulting in a five-pointed star-shaped complex. The designation of gold–gold attractive interactions in these species is not straightforward since it involves Au(I) atoms but, nevertheless, the metal–metal distances are significantly shorter in the mesityl bridged species ($d_{Au-Au} \approx 2.7$ Å) than in the CX_2-bridged species ($d_{Au-Au} > 2.9$ Å) [6]. When the bridging ligand allows the formation of a larger than three-membered ring, the Au–Au distances can be longer, depending both upon the nature of the donor atoms and upon steric constraints imposed by substituents.

In fact, although Au(I) has a d^{10} closed-shell configuration, attractive interactions between two Au(I) centres are well known and have been explained, on the basis of extended Hückel results, by the mixing of empty metal s and p orbitals into the d shell [2,7]. This phenomenon, described as "aurophilicity" [4], is below the Hartree–Fock limit by ab-initio calculations and attributed to relativistic and correlation effects [8]. The great number of recent publications dealing with this problem, such as ab-initio studies on $[(XAuPH_3)_2]$ dimers, a tetrahedral Au_4 cluster and AuL species resulting from gas-phase reactions [9], and also some on related Cu(I) (d^{10}) species [10], shows that this topic is still of considerable interest. A recent study of gold–gold interaction on gold–phosphine complexes with main group atoms [11] indicates that extended Hückel calculations are still useful as the basis of an analysis of gold–gold bonds.

In this work, extended Hückel calculations [12] are performed on model complexes to study the Au–Au interactions. Special attention is given to understanding the direct influence of the nature of the bridging ligand on the Au–Au bond strength, while other important factors, such as the formal oxidation state of the metal, and the effect of the ligand *trans* to the Au–Au bond on phosphine ylide binuclear complexes, are also addressed.

The resulting knowledge is applied to a tentative assignment of formal oxidation states for the different types of gold atom in two mixed-valence complexes, the tetranuclear $[Au_4(C_6F_5)_2\{(PPh_2)_2CH\}_2(PPh_3)_2](ClO_4)_2$ [13] and the hexanuclear $[\{(2,4,6\text{-}C_6F_3H_2)Au(CH_2PPh_2CH_2)_2Au\}_2Au(CH_2PPh_2CH_2)_2Au](ClO_4)_2$ [14], where oxidation states are not easily assigned.

2. Results and discussion

2.1. Bonding in low nuclearity gold(I) complexes with C and P donors

The presence of Au(I)–Au(I) attractive interactions is well documented and has been studied mainly in complexes of type **1a**, where two L–Au–L units are close enough [2,7]. Some of the simplest are formed when two bidentate ligands support the gold–gold bond, resulting in a cyclic structure, as in the eight-membered ring complexes **2**. The bridging ligands may contain carbon, sulphur or phosphorus donor atoms, one example being the carbon atom donor $(CH_2)_2PPh_2$, in the bis(ylide) complex $[\{Au\{(CH_2)_2PPh_2\}\}_2]$ [3]. Two of these structural units **2** can be bound [15] or fused together [16]. There is also a recent example of a mixed-metal complex of cobalt and gold in a distorted ten-atom cycle supported by a bidentate phosphine (dppm) [17].

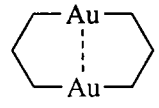

2

However, in all these compounds the gold–gold interactions may be constrained by the bidentate ligands, the corresponding bond distances ranging from 2.9 to 3.0 Å. The presence of chelating ligands in all these species somehow obscures the influence of the donor atom on the intermetallic bond strength, as each pair of gold atoms may be forced together into apparent bonding distances by the bite angle of the ligand.

In contrast, the existence of complexes of type **1b**, with open structures as shown in **3** and Au–Au distances longer than the previous distances ($d_{Au-Au} > 3.0$ Å), prompted us to look for metal–metal interactions and to compare the influence of carbon and phosphorus donors on the gold–gold bond strength.

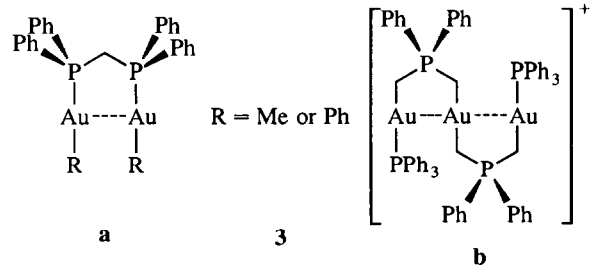

In the binuclear complex **3a**, the intermetallic distance is 3.15 Å for R = Me and 3.25 Å for M = Ph [18], and each gold atom is attached to one carbon and one

phosphorus atom. In the trinuclear complex **3b**, very long Au–Au distances of 3.39 and 3.54 Å are observed [19], but steric effects arising from the phenyl groups are responsible for this lengthening. Another geometrically similar trinuclear species for which this argument no longer holds, $[Au_3(\mu\text{-}PPh_2CH_2PPh_2)_2Cl_2]^+$, also exhibits Au–Au interatomic distances much greater than 3.0 Å (d_{Au-Au} = 3.07 and 3.16 Å) [20].

In these open-chain molecules **3**, the gold atoms are separated by distances longer than in the eight-membered ring species **2**. Their coordination sphere comprises at least one P atom, rather than only C donors.

Calculations were performed on simple model dimeric species **4**, differing in the number of carbon and phosphorus ligands, in order to study the gold–gold bond in this particular situation, and to determine the influence of the ligand donor atom type on the strength of the metal–metal bond. The geometrical parameters used in the models, as well as computational details of all the calculations, are given in the Appendix.

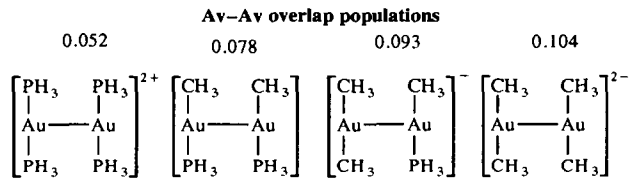

4

The gold–gold overlap populations (OPs) calculated for a fixed d_{Au-Au} = 2.8 Å increase with the number of carbon donors (from left to right in the structures **4**). As overlap populations directly reflect bond strengths, these values suggest that carbon ligands may indeed induce stronger Au–Au bonds. This is consistent with the tendency for shorter bonds to be associated with an increasing number of carbon ligands, as observed exper-

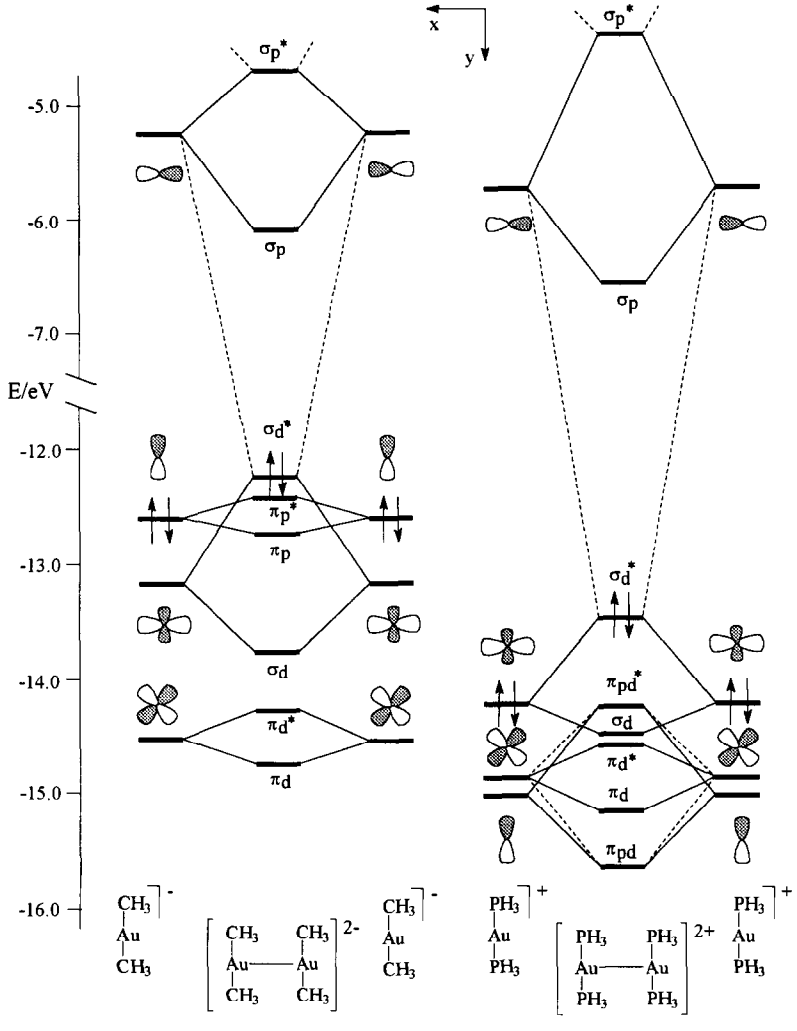

Fig. 1. Diagram of the interaction between two AuL_2 units in the Au_2L_4 gold(I) species $[Au_2(CH_3)_4]^{2-}$ (left) and $[Au_2(PH_3)_4]^{2+}$ (right).

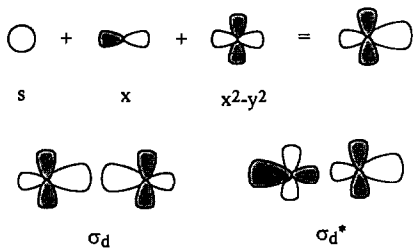

5

imentally. There are steric constraints in these models, owing to the close proximity of hydrogen atoms. This effect, which was studied in greater detail in a previous study [2], is essentially constant along the series and does not influence the general trends observed. For the staggered conformations of the ligands, the Au–Au overlap populations are very similar.

The well-known general features of the bonding between two L–Au(I)–L units [2] can also be found in Fig. 1, which applies to the two extreme cases of type **4** structures: $[Au_2(CH_3)_4]^{2-}$ and $[Au_2(PH_3)_4]^{2+}$. The main contribution to the intermetallic bonding, for both C and P donors, arises from the mixing of s and p with the $d_{x^2-y^2}$ orbital of each metal fragment. In the absence of s and p mixing, this would have produced a destabilizing four-electron interaction. Thus both Au–Au orbitals are stabilized: σ_d, with an enhancement of its bonding character, and the antibonding counterpart σ_d^*, which becomes almost non-bonding (**5**).

This general picture applies to ligands having either C or P donors. However, a closer look at the diagram in Fig. 1 reveals the difference between the two models. As the phosphorus donor orbital have lower energies than the corresponding carbon orbitals each AuL_2 fragment orbital will be comparatively stabilized for the phosphine complex. Since the orbitals involved in the Au–Au bonding (σ_d and σ_d^*) are L–Au–L antibonding orbitals, their energies will be lower when L is a P donor, resulting in a larger energy difference between the metal s and p_x levels and the d orbitals involved in the Au–Au bonding. This leads to a poorer mixing when the ligands are PH_3, and consequently to a weaker gold–gold bond, reflected by the composition of the σ_d^* orbital, which happens to be the highest occupied molecular orbital (HOMO) for both cases (Fig. 1). For $[Au_2(CH_3)_4]^{2-}$, it is composed of 37% of gold s and p_x (34% s and 3% p_x) and 25% of $d_{x^2-y^2}$ whereas for the phosphine model $[Au_2(PH_3)_4]^{2+}$, the gold s and p_x contribution drops to 23% (21% s and 2% p_x) and that of $d_{x^2-y^2}$ rises to 56%.

Another way of analysing these results is to look at the gold s and p_x electron occupancies. For the phosphine complex the s and p_x orbitals are populated with 0.768 and 0.035 electrons respectively, while for the CH_3 model those populations rise to 0.933 and 0.045, showing their increased involvement when L is a carbon donor.

The stabilization of Au–L orbitals for PH_3 complexes produces a secondary effect contributing to the weakening of the metal–metal bond. In fact, for $[Au_2(PH_3)_4]^{2+}$ (diagram on the right-hand side of Fig. 1), the metal p_y orbital is Au–L bonding and therefore so stabilized that it becomes close to d_{xy} and they both mix (orbitals π_{pd} and π_{pd}^* in Fig. 1), resulting in a strong destabilizing four-electron interaction.

These results suggest that Au–Au interactions in gold(I) species having phosphorus donors are expected to be weaker than in complexes having carbon donors, consistent with the fact that in the open-ring complexes **3** the Au–Au distances are longer than in complexes such as **2** where all ligands bind through carbon. Despite the small number of known complexes, the trend seems well defined. Nevertheless, the very large gold–gold distances observed for **3b** have their origin in the steric hindrance between neighbouring phenyl groups, rather than in an electron effect [19].

The striking gold complex with mesityl bridges, $[\{Au(Mes)\}_5]$ [5], which has a beautiful cyclic structure with alternating metal atoms and Mes bridges, producing a five-pointed star-shaped molecule (Fig. 2), is an example of a not very rigid structure having only carbon ligands and short Au–Au distances of about 2.7 Å.

This type of bridge has also been reported recently in a mixed gold and silver complex, where it spans asymmetrically each Au–Ag bond [21], and the mesityl group is closer to the gold atom.

In this work we focused our attention on species with a carbon atom bridging two gold(I) fragments. Besides the mesityl groups, Mes, only tetrahedral carbon groups CR_2 are observed in such roles, in polynuclear com-

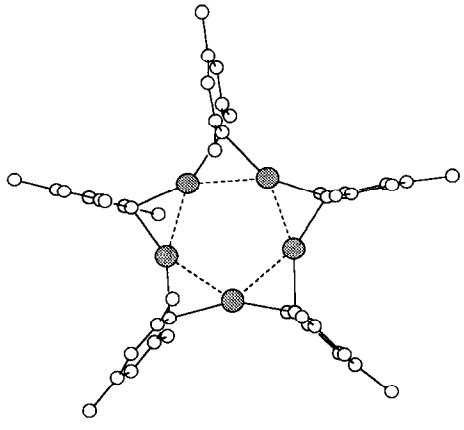

Fig. 2. Structure of $[\{Au(Mes)\}_5]$ (gold atoms are shaded and hydrogen atoms are omitted).

plexes where the resulting Au–Au distances are significantly longer (between 2.908 and 2.92 Å) [6].

Calculations were performed on two model complexes, one with an aryl bridge (C_6H_5), and the other with a tetrahedral carbon (CH_2), bridging two gold atoms, and also the real structures of both the Mes-bridged cluster [{$Au_5(Mes)_5$}] [5] and another containing a tetrahedral carbon bridge, [$SPPh_2C(AuPPh_3)_2PPh_2$-$CH(AuPPh_3)COOMe]ClO_4$ [6a]. The results were consistent. The OPs for structures **6** calculated for a fixed Au–Au distance, reveal a stronger interaction for the aryl-bridged species, consistent with the experimental data.

The bonding between each bridging group R and the metal fragment is depicted in Fig. 3 and consists of two donations from the bridging-ligand filled orbitals to empty metal orbitals, resulting in two R–metal bonds. There is a symmetrical interaction a_1 involving the carbon sp orbital pointing towards the middle of the

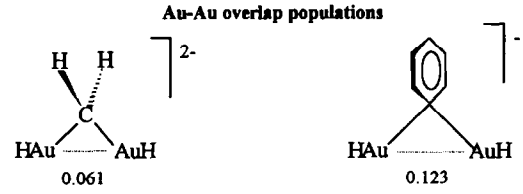

6

Au–Au bond, and the antisymmetrical counterpart b_1 with the carbon p orbital parallel to the metal–metal bond. The orbitals of the metal fragment involved are essentially symmetrical and antisymmetrical combinations of gold sp orbitals, since Au(I) has filled d orbitals.

The main difference between the bonding of the two bridging species lies in the antisymmetric interaction b_1. For methylene the orbital involved is a carbon pure p_x,

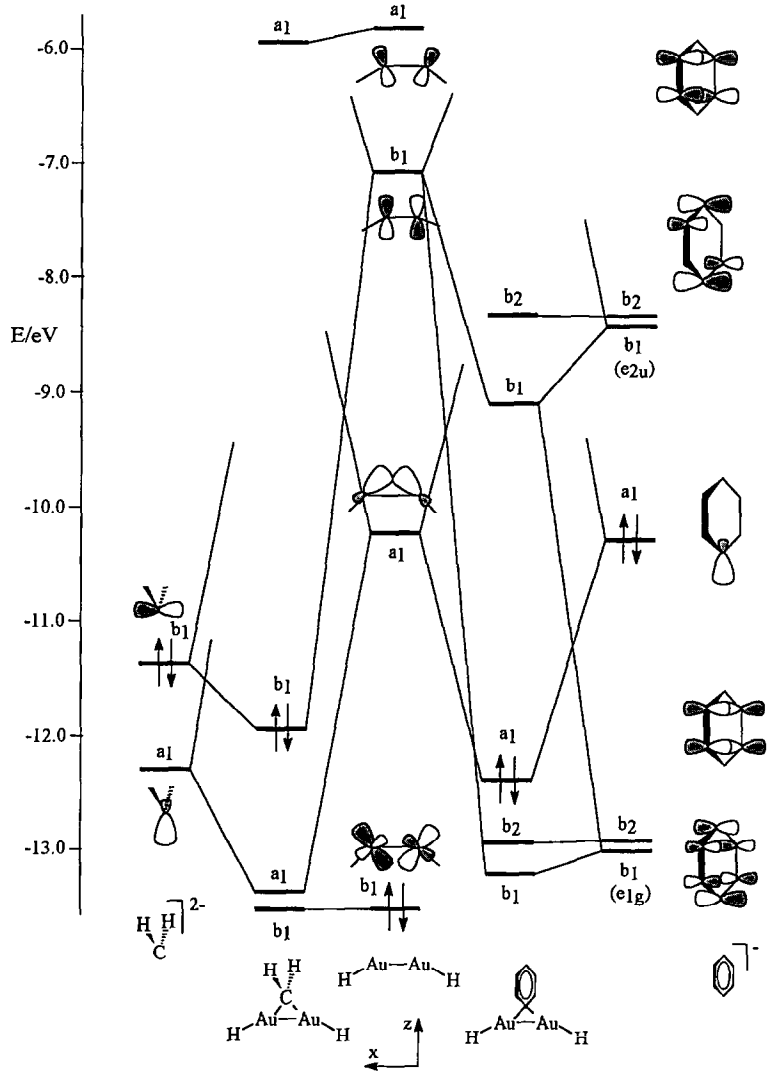

Fig. 3. Diagram of the interaction between a Au_2H_2 fragment (central) and a bridging CH_2^{2-} in the $[(\mu\text{-}CH_2)Au_2H_2]^{2-}$ complex (left), or a bridging $C_6H_5^-$ in the $[(\mu\text{-}C_6H_5)Au_2H_2]^-$ complex (right). The antibonding orbitals are not represented.

while for the phenyl group the b_1 donor orbital (one of the benzene e_{1g} set) is part of the ring π-aromatic system. So the corresponding bridging carbon p_x orbital is distributed among the six π orbitals and only "partially" involved in the R–Au bonding, as shown by the OP for the b_1 fragment orbitals: 0.180 for $R = C_6H_5$ and rising to 0.445 for the methylene-bridged species. The energy differences between these fragment orbitals reveal the same tendency, the b_1 donor orbital being significantly stabilized for the aryl ligand, and giving a poorer energy match with the metal b_1 (5.65 eV) than in the methylene case (4.25 eV).

The electronic consequence of bridge formation in either case is the partial filling of two metal-fragment orbitals. Although the population of the metal–metal bonding orbital a_1 enhances the intermetallic bond strength, the opposite effect arises when electrons are placed in the antibonding orbital b_1, the balance between these two factors determining the strength of the Au–Au bond in the bridged species. Thus, as the main difference between the bonding of the two bridging groups is the nature of the b_1 interaction, they will produce Au–Au interactions of different strengths in the final species, as the populations of the metal–metal antibonding orbital b_1 will be different. In fact, for the aryl bridging group this orbital receives 0.206 electrons, and when the bridging group is methylene that population rises to 0.492 electrons, justifying the Au–Au bond weakening in this case, and the accompanying bond elongation from about 2.7 to about 2.9 Å. In the case of alkyl bridges, this electronic effect leads to an Au–C–Au angle of 77° around the "tetrahedral" bridging carbon atom, as the distortion away from the normal bond angle is needed for the two gold atoms to approach each other.

The influence of the bridging group type on the metal–metal bond is also reflected in the bridge bonds Au–C in $R–Au_2L_2$. For the two examples studied, that bond is stronger for the methylene than for the aryl group, as shown by the OP between fragments (1.005 for $R = CH_2$ and 0.687 for $R = C_6H_5$) or by the $R–Au_2L_2$ binding energies (−4.6 eV for $R = CH_2$ and −3.6 eV for $R = C_6H_5$). The binding energies are the difference between the energy of the molecule and the sum of the energies of the two isolated fragments, namely the CH_2 or C_6H_5 group and the metal fragment. This is not surprising if we remember that in the methylene-bridged species both interactions between orbitals a_1 and b_1 are strong, while for the aryl-bridged complex the latter is much weaker. More simply, when two gold(I) atoms are bridged by a carbon atom, stronger Au–Au bonds are achieved at the expense of weaker C–Au bonds. This is consistent with the experimental C–Au distances between 2.13 and 2.20 Å for the Mes bridges in $[\{Au(Mes)\}_5]$ complex [5], and between 2.104 and 2.121 Å for the polynuclear species with CR_2 bridges [6].

2.2. Bonding in low nuclearity gold(II) and gold(III) complexes

There are a number of gold binuclear bis(ylide) complexes of type **7**, with the metal in formal oxidation states I, II or III, and different ligands X_1 and X_2 *trans* to the intermetallic bond. Some examples are given in Table 1.

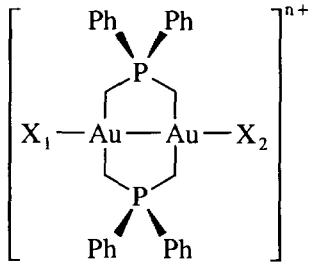

7

A brief analysis of the data in Table 1 shows a clear influence of the metal oxidation state on the Au–Au distance, the longest being found for the gold(III) com-

Table 1
Examples of dinuclear bis (ylide) gold complexes: experimental intermetallic distances and calculated overlap populations

Complex	X_1	X_2	*n*	d_{Au-Au} (Å)	Reference	Au–Au OP
Au(I) complex						
A $[Au(CH_2)_2PPh_2]_2$	—	—	0	2.98	[3]	0.104
Au(II) complexes						
B $[Ph_3PAu(CH_2PPh_2CH_2)_2AuPPh_3]^{2+}$	PPh_3	PPh_3	2	2.58	[22]	0.318
C $[Ph_3PAu(CH_2PPh_2CH_2)_2Au(C_6F_5)]^{+}$	PPh_3	C_6F_5	1	2.66	[23]	0.299
D $[(C_6F_5)Au(CH_2PPh_2CH_2)_2Au(C_6F_5)]$	C_6F_5	C_6F_5	0	2.68	[24]	0.295
Au(III) complex						
E $[(\mu\text{-}CH_2)\{Au(CH_2)_2PPh_2\}_2(C_6F_5)_2]$	C_6F_5	C_6F_5	0	3.11	[25]	0.029

plex **E**, which has a type **7** structure with an extra CH_2 group bridging the two gold atoms. The gold(I) species **A** has an intermediate Au–Au distance and the complexes **B–D** with gold in oxidation state II have the shortest Au–Au bond lengths.

A less obvious trend exists (Table 1). A closer analysis of Au(II)–Au(II) distances shows a slight but significant shortening with the increasing number of phosphines coordinated *trans* to the intermetallic bond.

All these differences in the nature and strength of the intermetallic bond are reflected by the calculated Au–Au OPs. The values reproduce the experimental distances well, indicating that electronic reasons associated with the Au–Au bond can, in principle, explain the structural differences.

Calculations on two model species, where X_1 and X_2 are two C or two P donors, were performed, aimed at understanding the *trans* influence of the phosphines on complexes **B–D**. The results are pictured in Fig. 4, where only the more significant interactions are shown.

The general features of the bonding are quite similar to those found for the interaction between two L–Au(I)–L fragments (Fig. 1), the main intermetallic bond interaction relying on the same $d_{x^2-y^2}$ orbital. Nevertheless, there are some important differences between the gold(I) and the gold(II) cases. Thus, whereas in the gold(I) species the metal–metal bond was achieved through s and p_x mixing with the $d_{x^2-y^2}$ orbital, as both the bonding (σ_d) and the antibonding (σ_d^*) molecular orbitals were occupied, for the gold(II) species that mixing still exists but is no longer the main contributor to the Au–Au bond. These complexes have two electrons less than the gold(I) complexes and the HOMO is σ_d, the antibonding σ_b^* being empty and becoming the

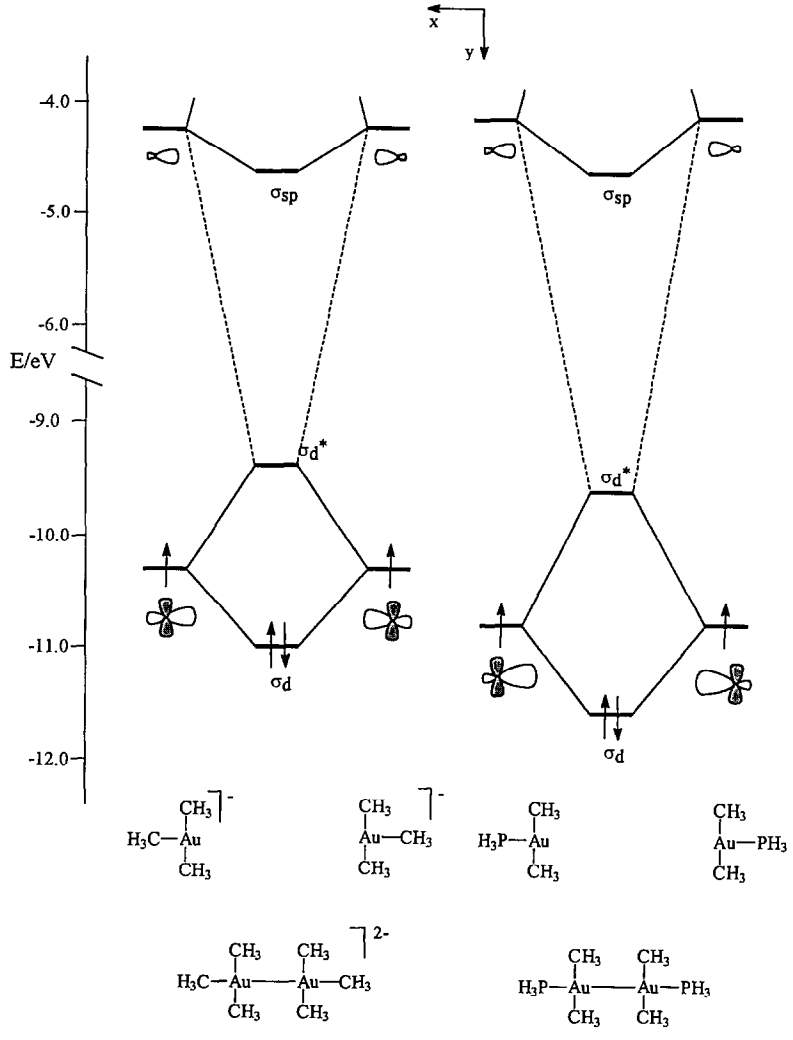

Fig. 4. Diagram of the interaction between two AuL_3 fragments in the gold(II) species Au_2L_6, $[Au_2(CH_3)_6]^{2-}$ (left) and $[Au_2(CH_3)_4(PH_3)_2]$ (right).

lowest unoccupied molecular orbital (LUMO) (Fig. 4). This explains the significant Au–Au bond length shortening on going from gold(I) to gold(II) complexes (see below).

A more subtle difference between the two cases lies in the nature of the fragment orbitals directly involved in the metal–metal bond. These are essentially $d_{x^2-y^2}$ in character but, whereas in the Au(I) species in Fig. 1 they are AuL_2 antibonding, in the Au(II) complexes there is an extra ligand L on each moiety. The antibonding AuL_3 character of the orbital is therefore increased, its energy being pushed up by about 3 eV. As the metal–metal bond is the result of the interaction of those orbitals, leading to the two molecular orbitals σ_d^* and σ_d, the nature of the ligands L has a direct influence on the Au–Au bond strength. This was observed for the Au(I) cases discussed above and also causes the change in intermetallic distances for the gold(II) complexes with different X_1 and X_2 ligands. Thus, the good energy match and overlap between the phosphorus orbitals and the metal orbitals previously discussed provides a more stabilized HOMO σ_d (about 0.7 eV) and consequently an enhanced Au–Au bonding character, whenever the ligands *trans* to the metal bond (X_1 and X_2) are phosphines. This result is clear from the comparison of both sides of the diagram in Fig. 4. The overlap population between the fragment orbitals responsible for the Au–Au bond is 0.264 when X_1 and X_2 are both carbon donors and rises to 0.307 for the phosphine derivatives, showing the stronger Au–Au bonding character of their σ_d orbital.

These results are consistent with the experimental distances given in Table 1 and explain the *trans* influence of the phosphine ligands on the Au–Au bond strength for the gold(II) complexes **B–D**. However, it should be noted that the differences found are small (Fig. 4), as are the differences in the intermetallic bond lengths (Table 1), 0.1 Å for the two extreme cases **B** and **D**. Unfortunately, the number of available complexes is very small and no statistical meaning can be attached to these values.

Experimental studies of the *trans* influence of the ligand in related complexes (X_1 and X_2 are an alkyl and a halogen respectively) showed that although the ligand has a strong influence on the Au–X bond length, the intermetallic distance remained almost unchanged [26].

Of the complexes presented in Table 1, the gold(III) complex **E**, which has a methylene group bridging the two metal atoms, exhibits the longest intermetallic distance.

The bonding between the bridging CH_2 and the Au_2 fragment is depicted in Fig. 5 and consists of two electron donations from the bridging carbene orbitals a_1 and b_1 to appropriate empty metal orbitals. These are the equivalent of σ_d and σ_d^* described for the gold(I)

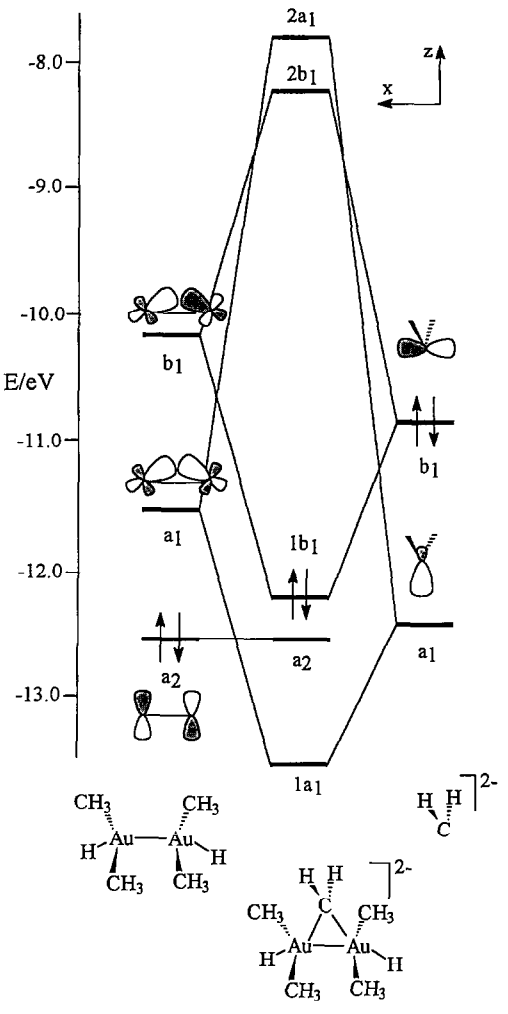

Fig. 5. Diagram of the interaction between a bridging CH_2^{2-} and a $Au_2(CH_3)_4(H)_2$ fragment in the complex $[(\mu\text{-}CH_2)Au_2(CH_3)_4(H)_2]^{2-}$.

and gold(II) species in Figs. 1 and 4 and are now both empty, as the metal oxidation state is III. The different symmetry labels arise from the C_{2v} symmetry of the model used in the calculations.

The symmetrical component of the bonding results from the interaction between the carbon sp orbital pointing towards the middle of the Au–Au bond (a_1) and the corresponding metal orbital (σ_d in Figs. 1 and 4). The antisymmetrical counterpart b_1 involves the carbon p orbital parallel to the Au–Au axis and the metal orbital corresponding to σ_d^* in Figs. 1 and 4. The overall result is the formation of two Au–C bonds and the partial filling of two empty metal orbitals.

We now have all the data needed to compare metal–metal bonds in gold(I), gold(II) and gold(III) complexes. The comparison between gold(I) and gold(II) compounds is straightforward. For Au(I), both metal–metal bonding and antibonding orbitals are filled (σ_d^* and σ_d in Fig. 1), and the only attractive interaction results from s and p mixing into the d orbitals. Calcula-

tions performed for **A** using coordinates taken from the real structure lead to a metal–metal overlap population of 0.043, indicating a weak Au–Au bonding interaction. On the contrary, for Au(II) derivatives (Fig. 4), only the metal–metal bonding orbital σ_d is occupied. The antibonding σ_d^* orbital remains empty, and therefore the Au–Au bond is stronger (OP, 0.295 for the model complex $[Au_2(CH_3)_6]^{2-}$).

Comparing Au(II) and Au(III) complexes is also easy, as for the latter there is only partial occupation of the two relevant orbitals. The Au–Au bonding orbital σ_d (a_1 in Fig. 5) gains 0.868 electrons, while the antibonding orbital σ_d^* (b_1 in Fig. 5) receives 0.772 electrons (OP, 0.029). Thus, for Au(III) species, there is only partial occupancy of the Au–Au bonding orbital which is filled for the Au(II) complexes. In addition, the antibonding orbital is also partially populated, but the equivalent orbital stays empty in the gold(II) compounds.

From these arguments, it is clear that gold(II) complexes have the strongest Au–Au bonds and the corresponding shorter distances, as only the Au–Au bonding molecular orbital is occupied.

The difference between Au(I) and Au(III) complexes **A** and **E** is, however, less obvious, because the two species have both metal–metal bonding and antibonding orbitals filled (Figs. 1 and 5). The answer lies in the nature of the σ_d^* orbital. For the Au(I) species there is no third ligand L coordinated *trans* to the Au–Au bond, so that the $d_{x^2-y^2}$ orbital involved in the metal–metal bonding is AuL_2 antibonding, and metal p_x mixes in such a way that the resulting σ_d^* orbital becomes almost non-bonding (**8a**). In contrast, in the Au(III) complex, the ligands X_1 and X_2 *trans* to the Au–Au bond imply that the orbital involved in the metal–metal bond is AuL_3 antibonding. The mixing of the metal p_x orbital has the opposite effect to that of the previous case, decreasing the Au–L antibonding character and enhancing the Au–Au antibonding character. As a result, σ_d^* becomes more antibonding for Au(III) complexes **8b**.

In other words, the Au–Au bond is stronger in the gold(I) complex **A** than in the gold(III) complex **E**, because the ligands X *trans* to the Au–Au bond in the latter produce a less effective s and p mixing into the d block, preventing better stabilization of the partially filled σ_d^* orbital.

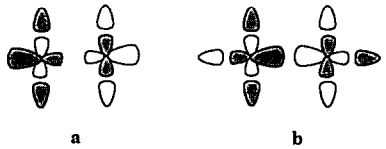

8

2.3. Gold–gold bonding and oxidation state assignment in mixed-valence complexes

The previous description of gold–gold bonds and the knowledge obtained can be applied to the assignment of formal oxidation states of gold atoms in some polynuclear clusters. This is not always a straightforward task, as sometimes a simple electron-counting scheme considering all the metal atoms identical will end up with non-integral oxidation states. This is the case for mixed-valence complexes, and the use of calculations to understand the electronic structure of these molecules can be a helpful tool.

As an example, the Au_5 complex $[[\{Au(CH_2)_2PPh_2\}_2\text{-}(C_6F_5)]_2Au(C_6F_5)_2]^+$ has five gold atoms in a chain with a 9 + total charge [27]. Previous calculations showed that the outer metals were involved in stronger Au–Au bonds, suggesting the following oxidation state distribution for the chain: Au(III)–Au(I)–Au(I)–Au(I)–Au(III). The charge distribution is consistent qualitatively with this [2].

The two new mixed-valence complexes with controversial oxidation states assignments for the various metal atoms prompted us to perform some calculations in order to understand the intermetallic bonding and to assign tentatively the various metal oxidation states.

The first of these species is closely related to the above-mentioned Au_5 chain and contains a linear Au_6 chain $[\{(2,4,6\text{-}C_6F_3H_2)Au(CH_2PPh_2CH_2)_2Au\}_2\text{-}Au(CH_2PPh_2CH_2)_2Au](ClO_4)_2$ [14], with three Au_2 bis(ylide) units. Its geometry is depicted in the structure **9**. The six gold atoms bear a total formal charge of 10 + .

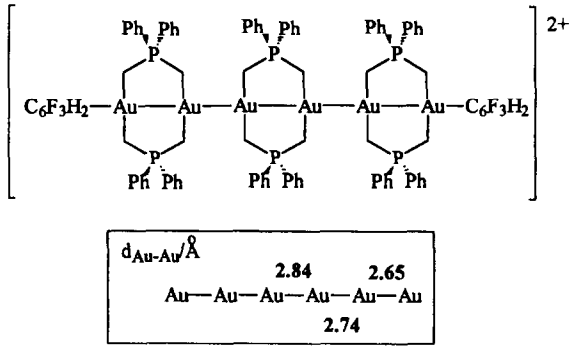

9

The second complex, $[Au_4(C_6F_5)_2\{(PPh_2)_2CH\}_2\text{-}(PPh_3)_2](ClO_4)_2$ [13], is tetranuclear and has a T frame arrangement of the metal atoms, three in a row, with the fourth interacting with the central atom. Its geometry is depicted in the structure **10**. In this case the metal fragment has a 6 + total charge.

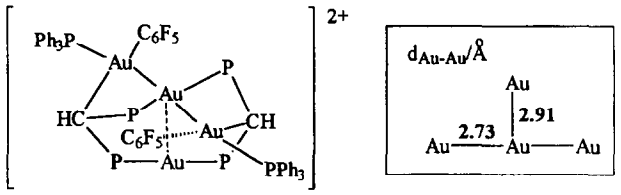

10

Calculations were performed on model complexes, and the results show that the outer atoms of **9** and **10** behave differently. These atoms have greater electron-deficient character and form stronger Au–Au bonds, as demonstrated by the experimental bond distances of **9** and **10** and the calculated OPs (**11**).

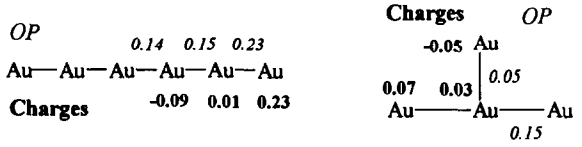

11

These results are similar to those found for the Au_5 chain [2], and as the bonding scheme is the same it will not be repeated here. Briefly, the inner atoms are more electron rich, with electron distributions close to Au(I) d^{10}, and they participate in weaker Au–Au bonds supported by s and p mixing. However, the outer metal atoms have empty d orbitals, and are able to form stronger intermetallic bonds, as in the simple dinuclear complexes discussed previously (Figs. 1 and 4).

The nature of the metal d orbital involved in the Au–Au bonding is responsible for the electronic differences found between the inner and the outer metal atoms. This orbital has AuL antibonding character and, as already discussed for the cases of Au(I) and Au(III) dinuclear bis(ylide) complexes **7**, the numbers of ligands L, coordinated to each metal atom have a direct influence on its composition. Only the outer atoms of **9** and **10** are AuL_3 units, all the others being AuL_2. Thus, whereas the inner atoms use AuL_2 antibonding orbitals for the Au–Au bonds, the outer atoms use AuL_3 antibonding orbitals with higher energies and consequently more likely to be empty (**12**).

The proposed formal oxidation-state distribution for **9** is then Au(III)–$[Au(I)]_4$–Au(III), and for **10** is Au(II)–Au(I)–Au(II) for the Au_3 chain, and Au(I) for the fourth atom. Although the latter assignment is with that proposed for **10** based on Au–Au distances and each metal coordination sphere [13], the same type of argument implies the assignment $[Au(II)]_2$–$[Au(I)]_2$–$[Au(II)]_2$ for the Au_6 chain **9**. One must bear in mind that these are mixed-valence species in which no clear unique oxidation state can be defined, and they are probably better described by a combination of assignments.

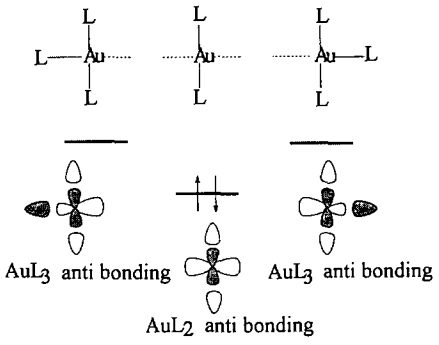

12

3. Conclusions

We tried to understand the electronic characteristics associated with Au–Au bonds in different coordination environments and metal oxidation states. In the binuclear bis(ylide) gold complexes, phosphine ligands induce stronger metal–metal bonds when coordinated *trans* to the Au(II)–Au(II) bond, and they have the opposite effect in gold(I) dinuclear compounds. Indeed, P ligands stabilize the metal orbitals involved in the Au–Au bonding, which results in a stronger intermetallic bond for gold(II) compounds, since only the bonding orbital is occupied. In contrary, in the case of gold(I) this same stabilization allows less s and p mixing into the occupied antibonding orbital, owing to poorer energy match.

The Au–Au bond strength of two Au(I) atoms bridged by one carbon atom, was found to be closely dependent on the ligand type, aryl ligands, such as mesityl, inducing stronger intermetallic bonds than tetrahedral carbon ligands, CR_2.

Mixed-valence polynuclear complexes were also addressed, and oxidation-state distributions proposed. The outer metal atoms of linear arrangements were found to be less electron rich and to participate in stronger Au–Au bonds, the reason being related to the number of ligands on each metal.

Appendix

All the calculations were done using the extended Hückel method [12] with modified H_{ij} values [28]. The basis set for the metal atoms consisted of *n*s, *n*p and $(n-1)$d orbitals. The s and p orbitals were described by single Slater-type wavefunctions, and the d orbitals were taken as contracted linear combinations of two

Slater-type wavefunctions. The parameters used for Au were for H_{ii} (eV), ζ as follows: 6s, −10.92, 2.602; 6p, −5.55, 2.584; 5d, −15.07, 6.163, 2.794 (ζ_2), 0.6442 (C_1), 0.5356 (C_2). Standard parameters were used for other atoms.

The calculations were performed on model complexes with idealized geometries taken from the real structures referenced in the text. Phenyl groups were replaced by hydrogen atoms and the bis(ylide), $(CH_2)PPh_2$, by two methyl groups, since the results were not qualitatively altered. The Au–Au bond distance was 2.8 Å for all the compounds, except for the Au_6 chain in which a 2.7 Å separation was used. The other bond distances were as follows: Au–C, 2.1 Å; Au–P 2.4 Å; Au–H, 1.7 Å, C–C, 1.4 Å; C–H 1.1 Å, P–H, 1.4 Å.

References

[1] F.H. Allen, J.E. Davies, J.J. Galloy, O. Johnson, O. Kennard, C.F. Macrae, E.M. Mitchell, J.M. Smith and D.G. Watson, *J. Chem. Inf. Comput. Sci., 31* (1991) 187.

[2] M.J. Calhorda and L.F. Veiros, *J. Organomet. Chem., 478* (1994) 37.

[3] J.D. Basil, H.H. Murray, J.P. Fackler, Jr., J. Tocher, A.M. Mazany, B. Trzcinska-Bancroft, H. Knachel, D. Dudis, T.J. Delord and D.O. Marler, *J. Am. Chem. Soc., 107* (1985) 6908.

[4] (a) H. Schmidbaur, *Gold Bull. 23* (1990) 11; (b) H. Schmidbaur, *Pure Appl. Chem., 65*, (1993) 691.

[5] E.M. Meyer, S. Gambarotta, C. Floriani, A. Chiesi-Villa and C. Guastini, *Organometallics, 8* (1989) 1067.

[6] (a) M.C. Gimeno, A. Laguna, M. Laguna, F. Sanmartín and P.G. Jones, *Organometallics, 12* (1993) 3984; (b) E.J. Fernández, M.C. Gimeno, P.G. Jones, A. Laguna, M. Laguna and J.M. Lopez-de-Luzuriaga, *Angew. Chem., Int. Edn. Engl., 33* (1994) 87.

[7] (a) Y. Jiang, S. Alvarez and R. Hoffmann, *Inorg. Chem. 24* (1985) 749; (b) P.K. Mehrotra and R. Hoffmann, *Inorg. Chem. 17* (1978) 2187; (c) K.M. Merz and R. Hoffmann, *Inorg. Chem., 27* (1988) 2120; (d) A. Dedieu and R. Hoffmann, *J. Am. Chem. Soc. 100* (1978) 2074; (e) D.M.P. Mingos, *J. Chem. Soc., Dalton Trans.*, (1976) 1163.

[8] (a) P. Pyykkö and Y.-F. Zhao, *Angew. Chem., Int. Edn. Engl., 30* (1991) 604; (b) P. Pyykkö, *Chem. Rev., 88* (1988) 563.

[9] (a) P. Pyykkö, J. Li and N. Runeberg, *Chem. Phys. Lett., 218* (1994) 133; (b) R. Boca, *J. Chem. Soc., Dalton Trans.*, (1994) 2061; (c) D. Schröder, J. Hrušak, R.H. Hertwig, W. Koch, P. Schwerdtfeger and H. Schwarz, *Organometallics, 14* (1995) 312.

[10] (a) A. Schäfer, C. Huber, J. Gauss and R. Ahlrichs, *Theor. Chim. Acta, 87* (1993) 29; (b) A. Schäfer and R. Ahlrichs, *J. Am. Chem. Soc., 116* (1994) 10686.

[11] J.K. Burdett, O. Eisenstein and W.B. Schweizer, *Inorg. Chem., 33* (1994) 3261.

[12] (a) R. Hoffmann, *J. Chem. Phys., 39* (1963) 1397; (b) R. Hoffmann and W.N. Lipscomb, *J. Chem. Phys., 36* (1962) 2179.

[13] M.C. Gimeno, J. Jiménez, P.G. Jones, A. Laguna and M. Laguna, *Organometallics, 13* (1994) 2508.

[14] A. Laguna, M. Laguna, J. Jiménez, F.J. Lahoz and E. Olmos, *Organometallics, 13* (1994) 253.

[15] (a) I.J.B. Lin, C.W. Liu, L.-K. Liu and Y.-S. Wen, *Organometallics, 11* (1992) 1447; (b) M. Bardají, N.G. Connelly, M.C. Gimeno, J. Jiménez, P.G. Jones, A. Laguna and M. Laguna, *J. Chem. Soc., Dalton Trans.*, (1994) 1163.

[16] V.W.-W. Yam, T.-F. Lai and C.-M. Che, *J. Chem. Soc., Dalton Trans.*, (1990), 3747.

[17] A. Pons, O. Rossell, M. Seco and A. Perales, *Organometallics, 14* (1995) 555.

[18] X. Hong, K.-K. Cheung, C.-X. Guo and C.-M. Che, *J. Chem. Soc., Dalton Trans.*, (1994) 1867.

[19] E. Cerrada, M.C. Gimeno, J. Jiménez, A. Laguna and M. Laguna, *Organometallics, 13* (1994) 1470.

[20] R. Usón, A. Laguna, M. Laguna, E. Fernandez, M.D. Villacampa, P.G. Jones and G.M. Sheldrick, *J. Chem. Soc., Dalton Trans.*, (1983) 1679.

[21] M. Contel, J. Jiménez, P.G. Jones, A. Laguna and M. Laguna, *J. Chem. Soc., Dalton Trans.*, (1994) 2515.

[22] R. Usón, A. Laguna, M. Laguna, J. Jiménez and P.G. Jones, *J. Chem. Soc., Dalton Trans.*, (1991) 1361.

[23] A. Laguna, M. Laguna, J. Jiménez, F.J. Lahoz and E. Olmos, *J. Organomet. Chem., 435* (1992) 235.

[24] H.H. Murray, J.P. Fackler, Jr., L.C. Porter, P.A. Briggs, M.A. Guerra and R.J. Lagow, *Inorg. Chem., 26* (1987) 357.

[25] M. Bardají, M.C. Gimeno, J. Jiménez, A. Laguna, M. Laguna and P.G. Jones, *J. Organomet. Chem., 441* (1992) 339.

[26] H.H. Murray, J.P. Fackler, Jr., and B. Trzcinska-Bancroft, *Organometallics, 4* (1985) 1633.

[27] R. Usón, A. Laguna, M. Laguna, J. Jiménez and P.G. Jones, *Angew. Chem., Int. Edn. Engl., 30* (1991) 198.

[28] J.H. Ammeter, H.-J. Bürgi, J.C. Thibeault and R. Hoffmann, *J. Am. Chem. Soc., 100* (1978) 3686.